Macromolecules
ARTICLE

Macromolecules **2010**, *43*, 8479–8487 **8479**
DOI: 10.1021/ma101821z

Oligo- and Polyfluorene-Tethered *fac*-Ir(ppy)$_3$: Substitution Effects

Qifan Yan, Kan Yue,† Chao Yu, and Dahui Zhao*

Beijing National Laboratory for Molecular Sciences, Department of Applied Chemistry and the Key Laboratory of Polymer Chemistry and Physics of the Ministry of Education, College of Chemistry, Peking University, Beijing 100871, China. †Current address: Department of Polymer Science, Akron University, Akron, OH 44325.

Received August 10, 2010; Revised Manuscript Received September 13, 2010

ABSTRACT: A set of conjugated oligo- and polyfluorene-tethered *fac*-Ir(ppy)$_3$ complexes were synthesized. In addition to steady-state absorption and emission, time-resolved emission spectroscopy was used to systematically study the correlation of photophysical properties with chemical structures. A chain length dependency study showed that both radiative and nonradiative triplet decay rates, as well as the phosphorescence quantum yield, decreased with increasing chain length of the appended oligofluorene. Notably, the complex with oligofluorene tethered to the pyridine para to phenyl ring possessed a substantially higher phosphorescence quantum efficiency and shorter lifetime than those of an isomeric complex with the oligofluorene linked to the phenyl ring para to pyridine. Nonetheless, both these two oligomer complexes exhibited an excited state of mixed MLCT (metal-to-ligand charge transfer) and LC (ligand-centered) transitions, whereas another isomeric complex having an oligofluorene appended to the phenyl ring para to the iridium ion exhibited a particularly long triplet lifetime (> 100 μs), indicative of a ^{3}LC excited state. A moderately high quantum yield (~0.5) was displayed by this ^{3}LC-featured phosphor. DFT calculations substantiated the proposition that the attachment of oligofluorene to Ir(ppy)$_3$ at different positions resulted in varied molecular orbitals, with different relative contribution of MLCT to the emissive excited state. Hence, photophysical properties such as radiative decay rate, lifetime, and quantum yield, etc., were all influenced by the substitution isomerism. As these results indicated that if short lifetime and fast radiative decay were desired, among different substitution patterns appending the conjugated chain to the pyridine unit was the most favorable. Thus, star-shaped complexes with an oligo- or polyfluorene tethered to each of the three pyridine units of Ir(ppy)$_3$ were prepared. In such a structure, the tris-cyclometalated iridium effected nearly complete intersystem crossing (ISC) in all three ligands across three fluorene units, without compromising the phosphorescence quantum yield. But the study showed that further extending the conjugated ligand resulted in partial ISC or even complete loss of capacity for ISC beyond a certain distance.

Introduction

Triplet emitting cyclometalated iridium(III) complexes have been extensively studied for various applications such as organic light-emitting diodes (OLED), solid-state lighting,[1,2] sensing devices,[3,4] biological labeling agents,[5] etc. Particularly, incorporating heavy-metal complexes with strong spin−orbital coupling (SOC) interaction into the emissive layer of OLEDs enables effective intersystem crossing (ISC) and hence harnessing of both singlet and triplet excitons for light emitting, thereby improving the internal quantum efficiency of the devices.[6] This research area has attracted great interests in the past few years. Among different metallophosphors, cyclometalated iridium(III) complexes excel with their high phosphorescence quantum yield,[7] broadly tunable emission color,[8] and optimal lifetime.[9,10] For fabrication of large-area devices, solution-processed polymer-based LEDs lends a more viable and economical technique compared to the costly vacuum deposition method.[11] Incorporation of small-molecule triplet emitting molecules into polymer matrices can be accomplished by physical blending (i.e., doping). However, this procedure would normally cause phase separation between the dopant and polymer host over time, which has greatly curtailed the device performance.

Covalently tethering organometallic phosphors to conjugated polymers or oligomers, either into the main chain or via side chains, has proven an effective and convenient protocol for alleviating phase segregation.[12−16] The backbone-modification approach maximally exploits the SOC of the heavy metal and amplifies the phosphorescence through π-conjugation. Previously, Holmes and co-workers studied a series of solution-processable phosphorescent oligo- and polyfluorenes that were covalently linked to Ir(ppy)$_2$(acac) (ppy = 2-phenylpyridyl and acac = acetoacetonate) at the chain terminal.[12] More recently, neutral *fac*-Ir(ppy)$_3$ has attracted great attention due to its good thermal and chemical stability, rapid radiative decay, and, most importantly, an impressive phosphorescence quantum yield.[7] Bryce and co-workers reported the photophysical and electroluminescent properties of a series of homoleptic oligofluorenylpyridine−iridium complexes, which were prepared via ligand exchange reactions of Ir(acac)$_3$ with oligomer ligands.[13a] Holdcroft et al. studied the photophysics of some polyfluorenes with Ir(ppy)$_3$ incorporated in the backbone.[15] Cao et al. investigated the electroluminescence of a triplet-emitting polyfluorene electrolyte containing Ir(ppy)$_3$ units in the main chain.[14b] An Ir(ppy)$_3$ derivative with a 5-bromo-2-(4-bromophenyl)pyridine ligand was employed as a comonomer in synthesizing polymers in the two systems. In addition to linear-chain ligands, a variety of dendritic ligands have also been designed and tethered to Ir(ppy)$_3$, which effectively reduced detrimental intermolecular aggregation and triplet−triplet annihilation.[17] Recently, Müllen et al. reported a series of very large polyphenylene dendrimer decorated Ir(ppy)$_3$.[2b]

*Corresponding author. E-mail: dhzhao@pku.edu.cn.

Published on Web 09/28/2010

Chart 1. Studied Oligofluorene-Tethered *fac*-Ir(ppy)$_3$ Complexes

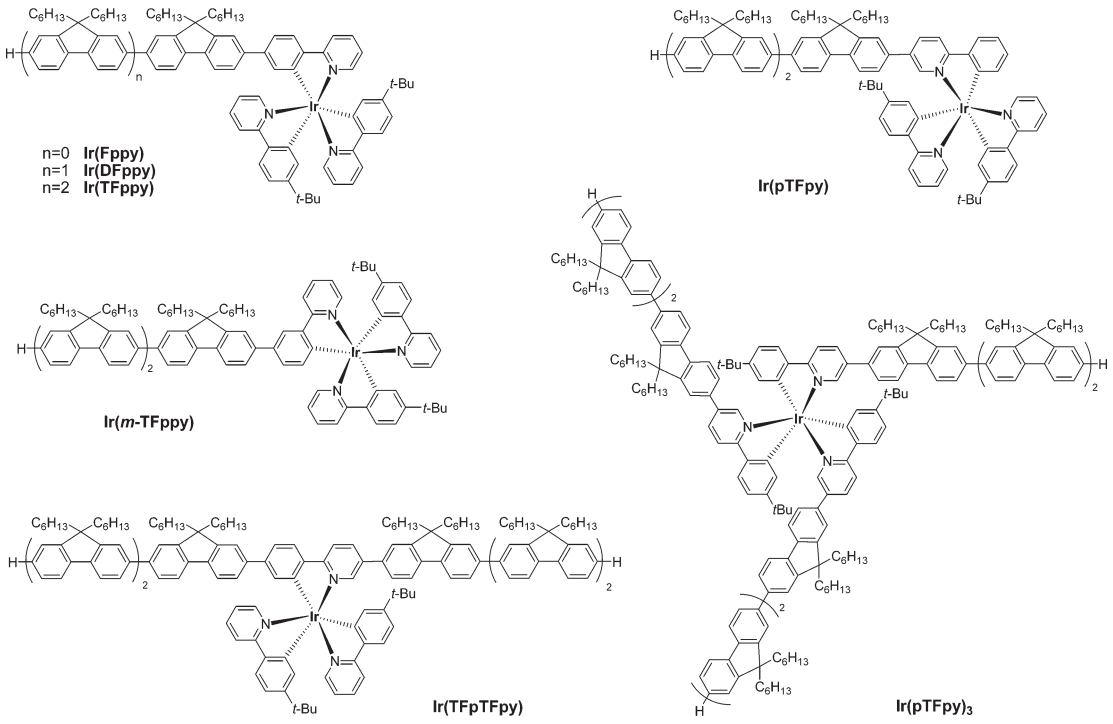

In addition to being applied in OLEDs, Ir(ppy)$_3$-containing polymers have recently been implemented in organic photovoltaics (OPV).[18] The longer lifetime of the triplet excited state compared to the singlet excited state is expected to influence both exciton migration distance and charge separation process. An increased external quantum efficiency was reported, attributed to the incorporation of a polyfluorene−Ir(ppy)$_3$ complex into the active layer of the device.

Although a number of Ir(ppy)$_3$-derived polymers and oligomers have been investigated, more detailed information and comprehensive understanding about the structure−property correlation of Ir(ppy)$_3$-based polymeric phosphors are yet to be acquired, as relevant knowledge is of great importance for rational design of molecules to suit varied applications. For example, for all different applications an optimal density of metal center bound to the polymer chain is necessarily to be identified, in order to most efficiently utilize the SOC effect. Overdosed metal centers will induce triplet−triplet annihilation, but an insufficient incorporation will result in incomplete ISC. Moreover, although the substituent effect has been investigated with small-molecule *fac*-Ir(ppy)$_3$ derivatives, complexes with conjugated chain structures tethered to different positions of ppy ligand have not been systematically compared and studied. Such structural variations should pronouncedly alter the photophysical properties, including the lifetime, quantum yield, decay rate, etc. These are critical factors governing the material properties and device performance. For example, in OLED a rapid radiative decay of the triplet exciton is preferred, but for sensing and imaging purposes a longer lifetime may be desired for higher sensitivity and convenient operation. In OPVs, a longer lifetime is also likely favorable for a longer exciton diffusion length and more effective charge separation.

The current contribution thus reports on a systematic investigation of the photophysical properties of *fac*-Ir(ppy)$_3$ tethered with oligofluorene at different positions of ppy (Chart 1). The system was selected because polyfluorene−Ir(ppy)$_3$-based materials are frequently used triplet phosphors in optoelectronics. Our study shows that not only the chain length of the oligofluorene but also, more importantly, the position at which the oligomer is tethered greatly alters the photophysics of the system. The phosphorescence lifetime can be tuned in the range of a few to tens of microseconds by simple substitution variation. Moreover, although the number of tethered oligomer chains does not considerably change the color of the emission, a brighter phosphorescence (per metal center) can be attained with a larger number of the oligomer ligands, resulting from greater absorbability of the oligomers and potent SOC of the iridium center.

Another accomplishment of the work is the attainment of a number of different bromo-substituted *fac*-Ir(ppy)$_3$ derivatives. With these newly acquired molecules, through various transition-metal-catalyzed coupling protocols, Ir(ppy)$_3$ units may now be conveniently incorporated to a variety of polymer chains in different substitution fashion. In the current report, the oligomer complexes were prepared via Suzuki cross-coupling of these bromo-substituted *fac*-Ir(ppy)$_3$ with oligofluorenylboronic acids. Other types of coupling reactions are also feasible with these bromo-substituted *fac*-Ir(ppy)$_3$ intermediates.

Results and Discussion

Syntheses of Oligomer Complexes. The syntheses of oligofluorene-tethered *fac*-Ir(ppy)$_3$ complexes are outlined in Schemes 1 and 2. First, five different Ir(ppy)$_3$ derivatives with mono- or dibromo-substituted ppy ligand(s) were prepared from corresponding chloride-bridged dimers via ligand exchange reactions facilitated by silver trifluoroacetate (Scheme 1). During the preparations of asymmetric complexes, Ir(BrpBrpy), Ir(Brppy), Ir(pBrpy), and Ir(*m*-Brppy), undesired ligand exchange was observed to occur with the ppy ligand originally present in the chloride-bridged dimer, in addition to that with the chloride anion. Hence, the target heteroleptic complexes had to be separated from byproducts using flash column chromatography. Initially, syntheses of brominated Ir(ppy)$_3$ derivatives without the *tert*-butyl substituents were attempted, but such compounds were difficult to purify due to the low solubility. The *tert*-butyl group was thus introduced for improving the solubility.[19] The *tert*-butyl-substituted complexes, exhibiting a better solubility, also allowed the ligand exchange reaction to be

Scheme 1. Syntheses of Bromo-Substituted *fac*-Ir(ppy)$_3$ Complexes

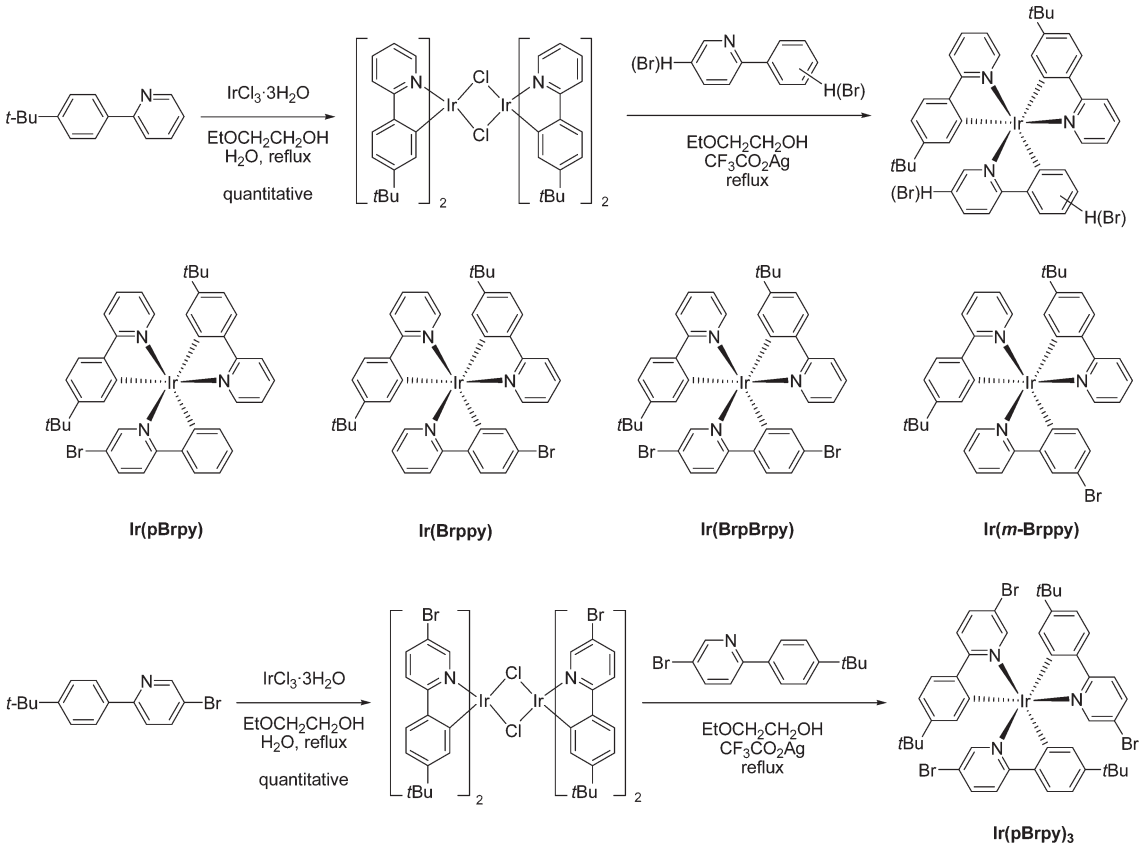

Scheme 2. Syntheses of Oligofluorenyl Ir(ppy)$_3$ Complexes

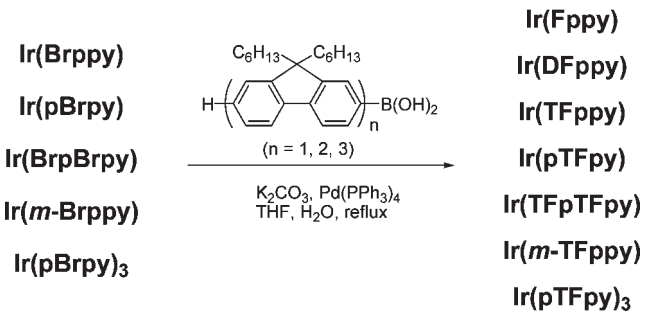

accomplished at a lower temperature, thereby minimizing the undesired ligand exchanges. The addition of silver trifluoroacetate further facilitated the reaction by forming AgCl precipitate.[20] Furthermore, the presence of the *tert*-butyl groups simplified the ^{1}H NMR spectra and helped identification of the product structures with NMR spectroscopy.

The homoleptic complex Ir(pBrpy)$_3$ was prepared following a similar procedure as those of the heteroleptic ones. Because of the C_3 symmetry, its facial configuration was easily identified by the simple appearance of the ^{1}H NMR spectrum (Figure 1).[10] The facial configuration of three heteroleptic complexes, Ir(BrpBrpy), Ir(Brppy), and Ir(pBrpy), was unambiguously verified by single crystal X-ray analyses (Figure 2).[21] The crystal structures revealed that substitution of hydrogen atom with bromine and/or *tert*-butyl groups did not significantly distort the molecular structure, as no pronounced deviation was observed with bond angle or bond length in substituted complexes from those of Ir(ppy)$_3$.[22]

All five bromo-substituted complexes, Ir(BrpBrpy), Ir(Brppy), Ir(pBrpy), Ir(*m*-Brppy), and Ir(pBrpy)$_3$, were then applied to Suzuki cross-coupling conditions to react with oligofluorenylboronic acid[23] to afford the oligomeric complexes. The structures of all seven obtained oligomer complexes (Chart 1) were characterized by ^{1}H NMR, MALDI-TOF, and elemental analyses (see the Supporting Information).

Absorption of the Oligomeric Complexes. UV−vis absorption spectra of all seven oligofluorenyl Ir(ppy)$_3$ were recorded in toluene at room temperature (Figure 3) and summarized in Table 1. Generally, the absorbance could be dissected into three parts: absorption of the oligomer ligand-centered (LC), spin-allowed S_0-S_1 ($\pi-\pi^*$) transition, with the shortest wavelength and largest extinction coefficient, that of the ^{1}MLCT (metal−ligand charge transfer) transition around 400−420 nm with a medium extinction coefficient, and that of the spin-forbidden ^{3}MLCT transition at ca. 450 nm with the smallest extinction coefficient. These absorption assignments are in accordance with those of a related set of oligomer complexes previously reported in the literature.[13a]

Compared with the prototype complex Ir(ppy)$_3$, the absorption of all oligomer complexes was dominated by the $\pi-\pi^*$ transition of the oligomer ligand. Not surprisingly, as the number of the attached fluorene unit increased from one to three in Ir(Fppy), Ir(DFppy), and Ir(TFppy), the absorption of this LC $\pi-\pi^*$ transition exhibited a progressive bathochromic shift, and the extinction coefficient escalated nearly in a linear correlation with the number of fluorene units (Figure 3a). Complexes Ir(TFppy) and Ir(pTFpy) displayed similar absorption features (Figure 3b), except for the slightly higher absorbability of the MLCT states for the latter. In spite of the meta linkage between the trifluorenylphenyl and pyridine unit in Ir(*m*-TFppy), it possessed slightly longer absorption wavelength than Ir(TFppy) and Ir(pTFpy). This indicated effective electronic coupling of

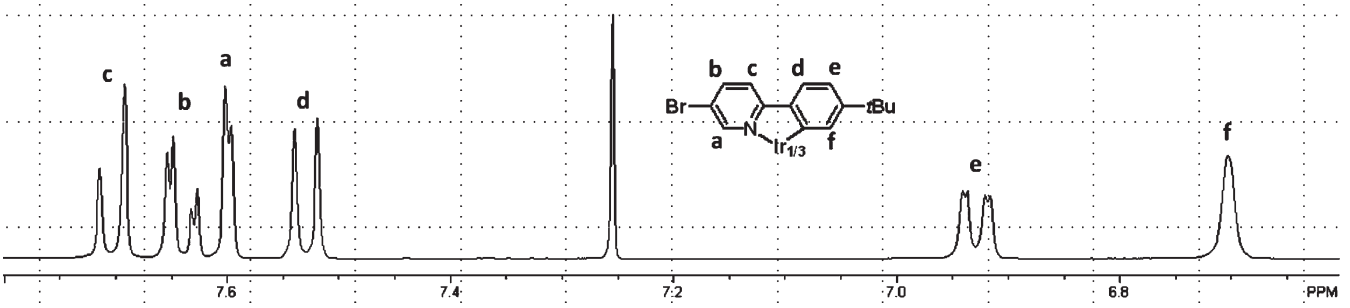

Figure 1. Aromatic region of the ^{1}H NMR ($CDCl_3$, 400 MHz) spectrum of homoleptic Ir(pBrpy)$_3$ with resonance assignment as indicated.

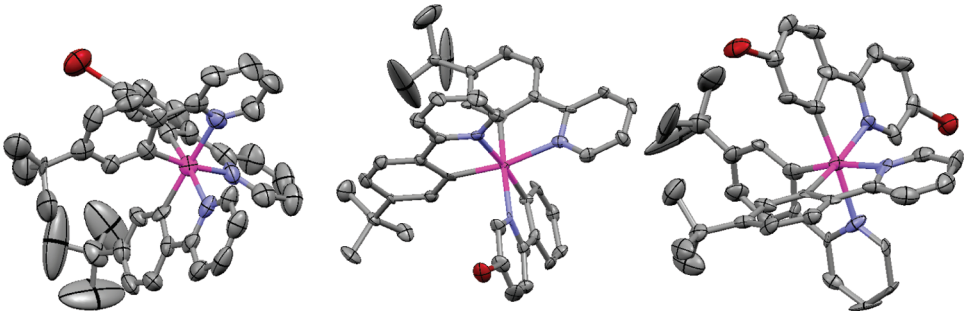

Figure 2. ORTEP drawings of Ir(Brppy), Ir(pBrpy), and Ir(BrpBrpy). The thermal ellipsoids represent 50% probability limit.

oligofluorene with the metal center (Figure 3b). Furthermore, Ir(pTFpy)$_3$ displayed very similar absorption band shape with that of Ir(pTFpy) except for the more than doubled extinction coefficient (Figure 3c). As expected, Ir(TFpTFpy) demonstrated the lowest $\pi-\pi^*$ absorption energy of all studied complexes, for it possesses the longest effective conjugation length in the oligomer ligand.

Steady-State and Time-Resolved Photoluminescence. Because of the very large SOC constant of iridium,[24] the rate of ISC is very rapid (typically < 100 fs) for small-molecule cyclometalated iridium complexes.[25] However, the question remains equivocal how effectively (far away) the SOC imparted by iridium ion could enable ISC in extended π-conjugated ligands. To obtain relevant information, the photoluminescence (PL) of the designed oligofluorenyl Ir(ppy)$_3$ complexes were systematically examined. All collected PL characterizations, including both steady-state and time-resolved data, are summarized in Table 1.

All the emission spectra were recorded in toluene by exciting at the absorption maximum, which corresponded to the spin-allowed LC $\pi-\pi^*$ transition of the oligomer complexes. Thus, singlet excitons should be generated initially in this process. Nonetheless, PL spectra revealed that phosphorescence dominated the emission for all the oligomer complexes, with negligible high-energy fluorescence emission (Figure 3). It thus indicated that nearly quantitative ISC took place in these systems. The emissions of all oligomer complexes were bathochromically shifted relative to that of Ir(ppy)$_3$. Notably, although the $\pi-\pi^*$ absorption maxima of Ir(DFppy) and Ir(TFppy) differed by 8 nm, these oligomers manifested very similar emission energy, which was lower than that of Ir(Fppy). This result verifies that triplet excitons are more localized compared to singlet excitons,[12a,13a,26] as their energy is no longer affected by the ligand chain length upon reaching two fluorene units. Nonetheless, Ir(TFppy) displayed no evident fluorescence, indicating that SOC interaction influenced at least three fluorene units. Alternatively, this may be explained by the fact that the singlet exciton initially generated in the system delocalizes over more than three fluorenyl units, which is evidenced by the continued bathochromic shift of the oligofluorene emission as the chain extends up to eight units long.[27]

Additionally, it was found that the phosphorescence quantum yield (Φ_p) dropped with the number of appended fluorene units increasing from 0 to 2 and then stabilized at 0.67, as Ir(DFppy) and Ir(TFppy) exhibited such an identical Φ_p value. With the time-resolved emission spectra, the phosphorescence lifetimes of Ir(Fppy), Ir(DFppy), and Ir(TFppy) were determined to be 4.1, 8.0, and 12 μs, respectively. In conjunction with Φ_p values, radiative and nonradiative decay rates from the triplet excited state were estimated for these oligomer complexes (Table 1). It was noted that, as the number of fluorene units attached to the phenyl ring (para to pyridine) increased from 1 to 3, both radiative and nonradiative decay rates (k_r and k_{nr}) attenuated. Specifically, the radiative decay was slower in these oligomer complexes than that in Ir(ppy)$_3$, but the nonradiative decay was faster than that in Ir(ppy)$_3$.

It is known that the HOMO of Ir(ppy)$_3$ comprises an admixture of the d orbital of the metal ion and π orbital of ppy, and its LUMO is mainly the π^* orbital of ppy with a major contribution from the pyridine moiety.[28] Thus, the T_1 state of the complex displays a nature of mixed MLCT and LC states. In Ir(Fppy), Ir(DFppy), and Ir(TFppy), the influence of the oligofluorene group over the ligand field strength should be insignificant, considering the meta linkage of the oligomer with respect to the C$-$Ir bond; therefore, the energy level of d orbitals should only be slightly affected by the presence of the oligofluorene. However, as the oligomer chain extended, the energy of LC $\pi-\pi^*$ transition decreased noticeably, with energy levels of π orbital increasing and π^* orbital decreasing due to more extended π-conjugation. With an elevated π orbital, the relative contribution from LC to the MLCT-LC mixed transition increased, resulting from a more effective mixing of the π-orbital with d orbital.[29] Accordingly, the relative contribution from MLCT was diminished.

Table 1. Absorption and Photoluminescence Properties of Oligofluorenyl Ir(ppy)$_3$ in Toluene

	absorption		photoluminescence					
compd	λ_{abs}[a]/nm	$\varepsilon/10^5$ M^{-1} cm^{-1}	λ_{em}[b]/nm	Φ_p[c]	τ[d]/μs	$k_r/\mu s^{-1}$	$k_{nr}/\mu s^{-1}$	$\Phi_p \times \varepsilon/10^5$ M^{-1} cm^{-1}
Ir(ppy)$_3$	378	0.14	510	0.97[e]	1.5	0.65	0.020	0.13
Ir(Fppy)	337	0.63	550	0.81	4.1	0.20	0.046	0.51
Ir(DFppy)	358	1.09	558	0.67	8.0	0.084	0.041	0.73
Ir(TFppy)	366	1.34	559	0.67	12	0.056	0.027	0.89
Ir(pTFpy)	364	1.26	568	0.82	4.2	0.20	0.043	1.03
Ir(*m*-TFppy)	370	1.03	524	0.50	114[f]	0.004	0.004	0.52
Ir(TFpTFpy)	378	2.31	591	0.64	4.9	0.13	0.073	1.48
Ir(pTFpy)$_3$	363	2.75	571	0.86	4.5	0.19	0.031	2.37

[a] Absorption maximum wavelength. [b] Emission maximum wavelength; the steady-state spectra were recorded by excitation at the absorption maximum, λ_{abs}. [c] Photoluminescence quantum yield measured with intersystem crossing efficiency assumed to be near unity, since negligible fluorescence was detected for the complexes; precision for Φ_p was ~5%. [d] Lifetimes were measured by time-correlated single-photon counting using NanoLED of 339 or 369 nm as the excitation source. [e] From ref 7a and this value was used as the standard for subsequent Φ_p measurements. [f] This long lifetime was determined by fitting phosphorescence decay curves generated by a pulsed Xe lamp to a single-exponential decay curve.

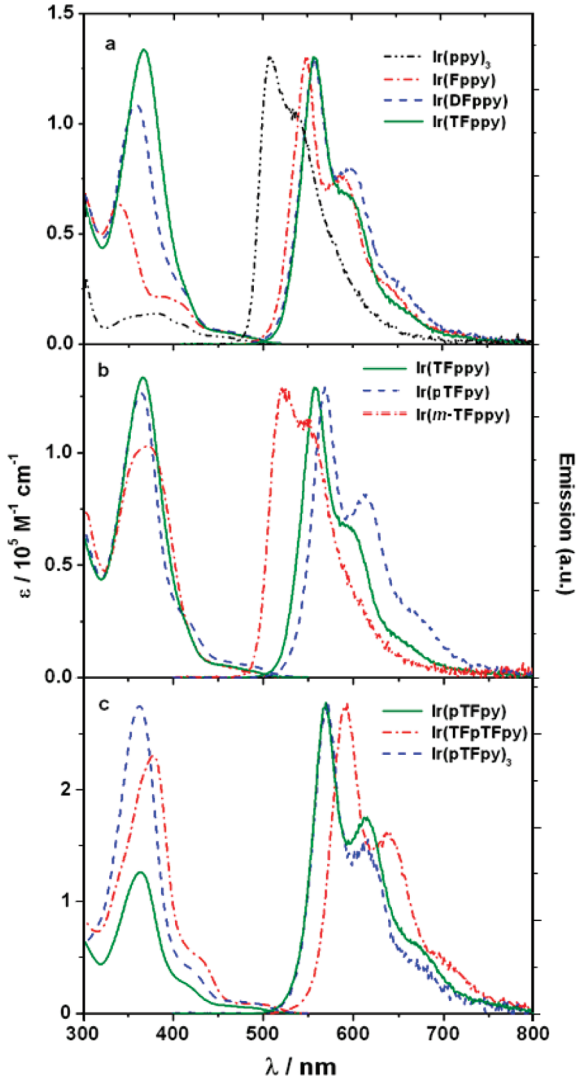

Figure 3. Absorption and normalized photoluminescence spectra of oligofluorenyl Ir(ppy)$_3$ complexes in toluene (absorption spectra were recorded at concentrations of ca. 1×10^{-5} M; emission spectra were recorded in degassed toluene solutions, excited at absorption maximum with O.D. of ca. 0.1).

This explains the decreased k_r with increasing oligofluorene chain length.

On the other hand, Ir(Fppy) exhibited a larger k_{nr} value compared to Ir(ppy)$_3$. This likely resulted from the decreased emission energy, as the energy gap law states that ln(k_{nr}) is inversely proportional to the emission energy.[30] Additional motional relaxation entailed by the attachment of a fluorene unit perhaps also contributed to the larger k_{nr}. However, further extension of the oligofluorene gave rise to decreased k_{nr}. This apparently was inconsistent with the energy gap law. A more plausible explanation is that the nonradiative decay is influenced by the same MLCT component as that governing the radiative transition, and thus the magnitude of k_{nr} showed a consistent trend with k_r.[31]

Subsequently, the regioisomeric effect was scrutinized regarding the position at which oligofluorene is attached to the ppy ligand. The PL maximum of Ir(pTFpy) is bathochromically shifted by about 10 nm relative to that of Ir(TFppy). Remarkably, a shorter lifetime (4.2 μs) and larger Φ_p (0.82) were manifested by Ir(pTFpy) than those of Ir(TFppy). Further examination unraveled the cause of such results was that k_r was more than tripled in Ir(pTFpy) compared with that in Ir(TFppy), while k_{nr} was less than doubled. The larger k_r, as well as k_{nr}, of Ir(pTFpy) is tentatively explained as follows. The pyridine unit plays a key role in accepting charge in the MLCT transition, which is reflected in the LUMO of Ir(ppy)$_3$ by showing a larger contribution from pyridine than from the phenyl moiety. The negative charge was likely better stabilized by delocalization when the trifluorenyl was tethered to pyridine compared to being tethered to the phenyl ring. Thus, the energy level of the MLCT state was lowered more pronouncedly in Ir(pTFpy), bringing about a larger contribution of MLCT to T_1 than that in Ir(TFppy).[32]

Interesting results also emerged from comparing the properties of Ir(*m*-TFppy) and Ir(TFppy). The structural variation in this pair of reigioisomers is that the trifluorenyl was switched from being para to the pyridine ring to para to iridium. A number of peculiar phenomena occurred from this structural alteration. First, although the absorption maximum of Ir(*m*-TFppy) displayed a slightly longer wavelength than that of Ir(TFppy), its phosphorescence maximum was hypsochromically shifted relative to that of Ir(TFppy) by 35 nm. More impressively, the phosphorescence lifetime of Ir(*m*-TFppy) reached over 100 μs. Its radiative decay was only 0.004 μs^{-1}, more than an order of magnitude smaller than that observed in Ir(TFppy). Such a lifetime value strongly suggests that, unlike those of Ir(TFppy) and Ir(pTFpy), the triplet excited state of Ir(*m*-TFppy) is of a dominant ^{3}LC feature, with a minimal contribution from MLCT, rendering particularly small k_r and k_{nr}. The origin of this LC-dominated excited state (rather than a mixed MLCT and LC state) in the chemical structure was analyzed. Since the trifluorene chain was tethered to the phenyl ring meta to pyridine, the π^* orbital of the oligomer was electronically decoupled from the pyridine moiety. But the MLCT transition intrinsically relies

on the electronegative pyridine unit to accept charge (electron) from the d orbital of the metal ion. Namely, in Ir(*m*-TFppy) the wave function of the MLCT state is localized on ppy unit, decoupled from the LC π^* orbital located on the oligofluorene chain, due to the meta linkage. Hence, the MLCT wave function was unable to perturb the ^{3}LC wave function, resulting in highly a spin-forbidden T_1 with a predominant ^{3}LC feature and slow radiative and nonradiative decays. The higher emission energy of Ir(*m*-TFppy) also served as supportive evidence for ineffective mixing of LC and MLCT wave functions. Ir(TFppy), with a more effectively mixed LC and MLCT, possessed a better stabilized T_1 and hence lower emission energy.

Such a long lifetime is rather rare for tris-cyclometalated Ir(III) complexes. With comparable k_r and k_{nr} values, Ir(*m*-TFppy) exhibited a phosphorescence quantum yield of ca. 0.5. A long lifetime in combination with a moderately high quantum efficiency, Ir(*m*-TFppy) may be a useful prototype molecule for designing phosphorescence sensors.

The photophysical properties of complex Ir(TFpTFpy) basically reflected mixed influences of the two trifluorenyl segments attached to the phenyl and pyridine rings. Although the emission energy became insensitive to ligand chain length in Ir(TFppy) and Ir(DFppy), further bathochromic shift emerged when another trifluorenyl was appended to the pyridine side (Figure 3c). Furthermore, complex Ir(TFpTFpy) manifested a k_r of an intermediate value between those of Ir(TFppy) and Ir(pTFpy). But k_{nr} was larger than those of both Ir(TFppy) and Ir(pTFpy), likely due to the lowered emission energy. This led to a slightly lower phosphorescence quantum yield in Ir(TFpTFpy) than that of Ir(TFppy).

Comparing the properties of Ir(TFppy), Ir(pTFpy), Ir(*m*-TFppy), and Ir(TFpTFpy), one may conclude that Ir(pTFpy) exhibited the most attractive features for application as electroluminescent materials, such as the shortest lifetime and highest Φ_p. Thus, a three-armed star-shaped, homoleptic oligomer complex Ir(pTFpy)$_3$ was subsequently synthesized by reacting homoleptic tribromo-substituted Ir(ppy)$_3$, Ir(pBrpy)$_3$, with a trifluorenylboronic acid. This oligomer complex, with a C_3 symmetry factor, had a total of nine fluorene units tethered around the iridium center and hence possessed a particularly enhanced absorbability. Moreover, it exhibited a similar k_r value with that of Ir(pTFpy) but a slightly slower nonradiative decay, resulting in a slightly longer lifetime but a higher quantum yield of 0.86.

As the extinction coefficient, ε, represents the ability of a molecule to absorb light at a given wavelength and Φ_p reflects its efficiency at converting the absorbed exciton into phosphorescence, ε times Φ_p may thus be used as an index to evaluate the capacity of a molecule at harvesting exciton and converted it into radiative energy (per iridium center). From the data shown in Table 1, it is evident that all of the synthesized oligomer complexes possess a larger value of ($\varepsilon \times \Phi_p$) than that of Ir(ppy)$_3$. Ir(pTFpy)$_3$ exhibits the largest value of ($\varepsilon \times \Phi_p$), which is ca. 18 times that of Ir(ppy)$_3$. Accordingly, the extended "arms" will be useful for collecting excitons in electroluminescence devices. In combination with its optimal lifetime, high quantum yield, and potentially good compatibility with host matrices, such a three-armed star-shaped complex structure is particularly advantageous for being applied as a triplet emitting dopant in OLED. Additionally, its unique C_3-symmetric star shape shares the structural advantage of dendron-decorated Ir(ppy)$_3$ in that the emissive center is relatively shielded by the extended ligands, thereby minimizing the detrimental quenching effect of nonemissive intermolecular aggregate formation in the condensed state.[2b,17]

Calculation of the Molecular Orbitals. Theoretical calculations were carried out to examine the molecular orbitals (MO) of these oligomer complexes in order to gain more in-depth understanding about the correlation of photophysical properties with the chemical structures. DFT calculations were conducted using Gaussian03.[33] Molecular geometry optimization and MO energies were calculated using the B3LYP hybrid functional[34] with 6-31G** basis set for C, H, and N atoms[35] and the "double-ζ" quality LANL2DZ basis set for Ir atoms.[28,36] In the calculations the hexyl groups at the 9-position of fluorenes were replaced with methyl groups for saving calculation time. The calculation results were very informative and consistent with our above speculations about the influences of MOs over the photophysical properties (Figure 4).

First, the trend of bandgap variation upon oligofluorene attachment, based on the calculated energy levels of frontier orbitals, qualitatively agreed with the experimentally observed emission energy. Specifically, of the three regioisomers, Ir(TFppy), Ir(*m*-TFppy), and Ir(pTFpy), Ir(pTFpy) exhibited the narrowest bandgap (i.e., energy difference between HOMO and LUMO), whereas Ir(*m*-TFppy) displayed the largest bandgap of all. Additionally, among different complexes LUMOs varied in energy to a much greater extent than HOMOs. Ir(pTFpy) showed a lower LUMO compared to that of Ir(TFppy), while Ir(*m*-TFppy) displayed a LUMO of highest energy.

Examining the configurations of frontier orbitals of Ir(TFppy) and Ir(pTFpy) in comparison with that of Ir(ppy)$_3$, it was found that only a very limited extent of delocalization to the tethered fluorenyl units occurred to HOMO, but a substantial portion of the LUMO was delocalized onto the oligomer part, which explains why the calculated energy of HOMOs showed minimal variation but LUMO exhibited much greater disparity in energy. Since the HOMO was relatively localized in Ir(TFppy) and Ir(pTFpy), the d orbital of the metal ion remained a major component of the HOMO. This ensured a significant contribution of MLCT to the admixture with LC, which is consistent with the fast decay rates observed with Ir(TFppy) and Ir(pTFpy). A much lower LUMO of Ir(pTFpy) relative to that of Ir(TFppy) confirmed our previous hypothesis that a more significant mixing of MLCT with LC occurred in this complex. This larger mixing was attributed to a more pronouncedly lowered MLCT state of Ir(pTFpy) (vide ante), which brought about a better stabilized T_1 with a greater component of MLCT.[32] Evidently, compared to the phenyl unit, being more electronegative and making a greater contribution to the LUMO, the pyridine unit in ppy is more critical in determining the stabilities of the MLCT transition and T_1 state.

Compared with those of Ir(TFppy) and Ir(pTFpy), the frontier orbitals of Ir(*m*-TFppy) displayed much distinct characteristics. The HOMO of Ir(*m*-TFppy) is significantly delocalized, with a considerable contribution from the oligofluorene portion. This difference in HOMO necessarily resulted from the fact that in Ir(*m*-TFppy) the trifluorene is attached to the iridiuim ion via a *p*-phenylene linker, which effected stronger electronic coupling. The calculation also indicated that Ir(*m*-TFppy) possessed a more elevated HOMO than Ir(TFppy) and Ir(pTFpy). This prediction was confirmed by electrochemical characterizations (Table S1), which revealed an evidently lowered oxidation potential of Ir(*m*-TFppy) relative to those of Ir(TFppy) and Ir(pTFpy). Imaginably, compared to Ir(TFppy) and Ir(pTFpy), the HOMO of Ir(*m*-TFppy) contains a smaller d orbital component due to such a greater extent of delocalization. Unlike the LUMO of Ir(TFppy) and Ir(pTFpy), the pyridine unit made hardly any

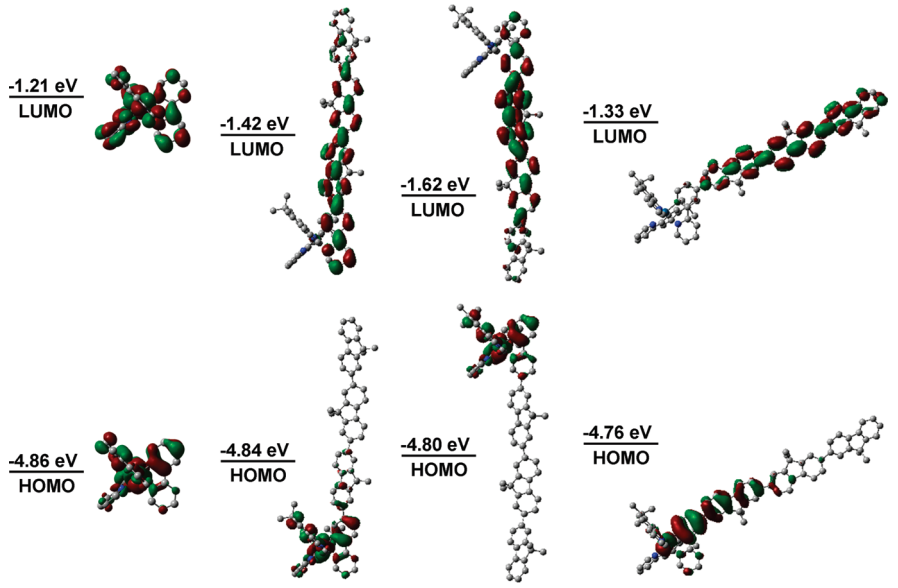

Figure 4. Calculated frontier MOs (LUMO, upper; HOMO lower) of Ir(ppy)$_3$, Ir(TFppy), Ir(pTFpy), and Ir(*m*-TFppy) (from left to right).

Scheme 3. Synthesis of Star-Shaped Polyfluorene-Substituted Ir(ppy)$_3$

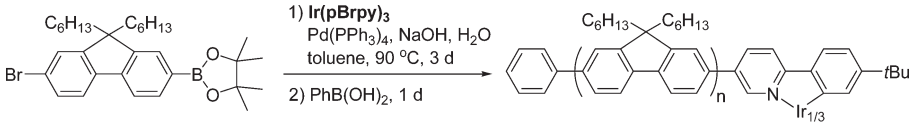

Ir(pPFpy)$_3$

contribution to the LUMO of Ir(*m*-TFppy). This necessarily resulted from the fact that in Ir(*m*-TFppy) the trifluorenyl is attached to the phenyl ring meta to pyridine. This meta position is a nodal point in the LUMO of Ir(ppy)$_3$. Conceivably, the LUMO of such an oligomer-tethered complex could either resemble the LUMO of Ir(ppy)$_3$, localized on ppy, or the π^* orbital of the oligofluorene, depending on which is lower in energy. The latter case was adopted by Ir(*m*-TFppy), suggesting a lower energy level of the π^* orbital of trifluorene in this complex. This calculation result well explained the experimental observation that T_1 of Ir(*m*-TFppy) manifested a particularly long lifetime and fairly low radiative decay rate, reflecting a LC-dominated T_1 state. Because of the lack of participation of the electronegative pyridine moiety, the LUMO of Ir(*m*-TFppy) was much higher energy in comparison with those of Ir(TFppy) and Ir(pTFpy), causing a hypsochromic shift of the emission.

Although Ir(TFpTFpy) exhibited a slightly lower LUMO (Figure S8) than that of Ir(pTFpy), it may not necessarily result from a more stabilized MLCT state. More likely, it was caused by a considerably lowered π^* orbital of the bis-(trifluorenyl)-substituted ppy ligand. Correspondingly, this complex exhibited a slower radiative decay rate, in comparison with that of Ir(pTFpy), consistent with a T_1 comprising a relatively smaller contribution of MLCT.

Synthesis and Photophysical Characterizations of a Star-Shaped Polyfluorene−Ir(ppy)$_3$ Complex. Since the three-armed star-shaped oligomer complex Ir(pTFpy)$_3$ exhibited desirable properties such as short lifetime, rapid radiative decay, and high quantum yield, a star-shaped polyfluorene-tethered homoleptic Ir(ppy)$_3$ complex was subsequently synthesized, using a modified procedure from the literature.[12a] A monomer bearing both aryl bromide and boronic acid functional groups, 2-(4′,4′,5′,5′-tetramethyl-1′,3′,2′-dioxaborolan-2′-yl)-7-bromo-9,9-dihexylfluorene, was treated with Ir(pBrpy)$_3$ under conditions that facilitate Suzuki cross-coupling reaction (Scheme 3). 30 equiv of bromofluorenylboronic acid relative to Ir(pBrpy)$_3$ (10 equiv per bromopyridyl unit) was added to the polymerization system. The polymer chain end was terminated with a phenyl group by adding an excess amount of phenylboronic acid to the reaction system after the polymerization proceeded for 3 days. The molecular weight (MW) of the resultant polymer complex was first characterized by gel permission chromatography (GPC), calibrated with monodispersed polystyrene standards. Number-averaged MW (M_n) was estimated to be 19.5 kDa for the obtained polymer (PDI = 2.1). The M_n was also evaluated using ^{1}H NMR spectroscopy by calculating the integration ratio of the resonance assigned to the aromatic hydrogen at the para position of C−Ir bond (δ = 7.0 ppm) to that of the first CH_2 unit in the hexyl side chains on the fluorene moieties (δ = 2.2 ppm). The number of fluorene units appended to each arm was thus estimated to be ~7. The discrepancy in the MWs calculated using GPC and NMR techniques may be ascribed to the fact that the polyfluorene-tethered Ir(ppy)$_3$ complex has a rigid structure, rather than being a flexible chain molecule.

The absorptions of Ir(pPFpy)$_3$ recorded in both solution and drop-cast thin film (Figure 5) were dominated by a band at ca. 380 nm, corresponding to the spin-allowed, LC $\pi-\pi^*$ transition. Relative to this strong absorption, the MLCT band subsided to near the baseline. The PL spectrum of the polymer recorded in toluene showed two major bands. The one of higher energy (around 420 nm) was ascribed to the fluorescence emission, since its intensity was insensitivity to oxygen and lifetime was of the order of nanoseconds. The other emission band of lower energy was sensitively quenched by oxygen and attributed to triplet excited state emission. Its wavelength (550−700 nm) and lifetime were similar to those of the phosphorescence emitted by Ir(pTFpy)$_3$. Time-resolved emission spectroscopy revealed a biexponential decay of the fluorescence at 414 nm, with two lifetime components being

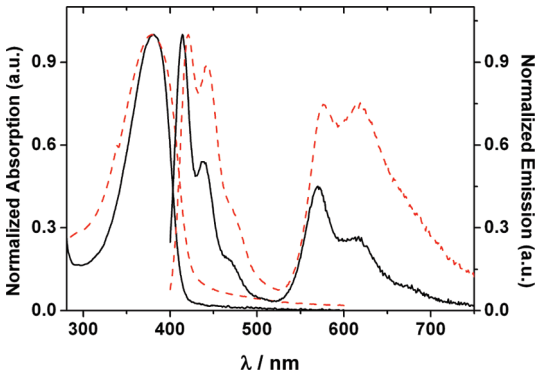

Figure 5. Normalized absorption and emission spectra of $Ir(pPFpy)_3$ in degassed toluene (solid lines) and drop-cast film (dashed lines).

Table 2. Photophysical Characterizations of $Ir(pPFpy)_3$

λ_{abs}/nm (ε/L g^{-1} cm^{-1})	380 (87)
λ_{em}/nm (in aerated toluene)	414
λ_{em}/nm (in degassed toluene)	414, 570[a]
λ_{em}/nm (drop-cast film)	423, 575

[a] Lifetimes: 0.44 ns (45%) and 0.14 ns (55%) at 414 nm; 4.6 μs at 570 nm.

0.44 ns (45%) and 0.14 ns (55%) (Table 2). The longer lifetime component agrees well with the lifetime of the fluorescence from a free oligofluorene.[37] The existence of a shorter lifetime component suggested a partial quenching of the singlet excited state. Presumably, ISC to the triplet state accounts for the major cause of this quenching. In conjunction with the observation that a nearly complete quenching of the fluorescence was observed with $Ir(pTFpy)_3$, such a biexponential decay of the fluorescence implied a dual singlet exciton decay pathway. Namely, when the ligand chain is short, the singlet excitons are always generated near the iridium ion where the SOC is effective; thus, rapid and complete ISC ensues. When the chain extends to a medium length, the influence of SOC subsides, and only a certain portion of the singlet excitons undergo ISC, giving rise to a partially quenched fluorescence with a reduced lifetime. Particularly, singlet excitons are able to migrate a certain distance within its inherent lifetime, and the direction of migration is random. Hence, some of the excitons migrated close to the iridium ion and underwent ISC, while others did not and decayed either radiatively or nonradiatively from S_1. If the chain length extends further, singlet excitons that are generated far away from iridium ion will have no chance to migrate to the vicinity of iridium within its lifetime; consequently, they may decay through fluorescing with an inherent lifetime.

Compared with the emission in solution, in drop-cast films the intensity of the phosphorescence of $Ir(pPFpy)_3$ was found to increase relative to that of the fluorescence. This could result either from a partial quenching of the fluorescence in the film or from the intermolecular energy transfer in thin films that assisted more singlet excitons to experience SOC and emit phosphorescence upon ISC, or perhaps from both. Imaginably, the phosphorescence intensity is sensitive to the film thickness. Thicker films emit stronger phosphorescence due to the limited oxygen permeability into the films.

Conclusion

A set of conjugated oligo- and polyfluorene-tethered $Ir(ppy)_3$ derived complexes were synthesized and studied regarding the correlation of photophysical properties with structural variation, using both steady-state and time-resolved spectroscopies. Important conclusions were drawn from comparing the properties of analogous oligomer complexes. First, the chain length dependence study confirmed that triplet excitons were more localized compared to singlet excitons. Both radiative and nonradiative decay rates decreased with increasing fluorene chain length, giving rise to an increased lifetime. Phosphorescence quantum yield also decreased with increasing chain length. More importantly, it was found that the oligomer complex having a trifluorene tethered to the pyridine ring gave substantially higher phosphorescence quantum yield and shorter lifetime than those of the isomeric complexes with oligofluorene tethered to the phenyl ring. Additionally, distinct properties were exhibited by regioisomers with an oligofluorene chain attached to different positions of the phenyl ring. When the trifluorene was appended to the phenyl ring para to the iridium ion, the lifetime of the triplet excited state prolonged to over 100 μs, characteristic of a ^{3}LC transition, while a moderate quantum yield was maintained. To our best knowledge, this is the longest lifetime so far reported for an $Ir(ppy)_3$ derivative. Calculated frontier orbitals of these oligomer complexes provided further insight into the photophysical features and their correlations with the chemical structures. Essentially, attachment of oligofluorene to different positions of ppy altered the relative contribution of MLCT to the T_1 state, mainly by modulating the π and π^* orbitals of the π-conjugated ligand(s). Moreover, a star-shaped oligomer complex with a trilfuorenyl appended to each of the pyridine units showed a higher phosphorescence quantum yield and shorter lifetime than an analogous complex with trifluorene tethered to both phenyl and pyridine rings of a ppy ligand. Finally, a polydispersed, three-armed star-shaped polymer complex was synthesized, which emitted both fluorescence (from the $\pi-\pi^*$ transition of the polyfluorenyl ppy ligand) and phosphorescence. On the basis of the detected biexponential decay of the fluorescence, a dual deactivation mechanism was proposed for the singlet excited state. Depending on the ligand chain length and the position the singlet exciton is generated at, it may or may not be affected by the SOC induced by iridium ion. In summary, appending the conjugated chains to the pyridine unit is favorable, compared to substituting the phenyl ring, if short lifetime and rapid radiative decay are desired. On the other hand, extending the conjugation by substituting the phenyl ring *para*- to iridium ion offers materials of a LC-dominated triplet state with a particularly long lifetime, while maintaining a moderately high quantum yield. These results are of great values for designing various $Ir(ppy)_3$-based triplet-emitting polymers.

Acknowledgment. This work is supported by the National Natural Science Foundation of China (Projects 20774005 and 50603001), the Ministry of Science and Technology of China (No. 2006CB921600), and Fok Ying-Tung Educational Foundation (No. 114008).

Supporting Information Available: Syntheses, experimental details, electrochemical data, and more calculated MOs. This material is available free of charge via the Internet at http://pubs.acs.org.

References and Notes

(1) (a) Thompson, M. E.; Djurovich, P. I.; Barlow, S.; Marder, S. R. In *Comprehensive Organometallic Chemistry*; O'Hare, D., Ed.; Elsevier: Oxford, 2007; Vol. *12*, pp 101−194. (b) *Highly Efficient OLEDs with Phosphorescent Materials*; Yersin, H., Ed.; Wiley-VCH: Berlin, 2007. (c) Yersin, H. *Top. Curr. Chem.* **2004**, *241*, 1–26. (d) You, Y.; Park, S. Y. *Dalton Trans.* **2009**, 1267–1282. (e) Wong, W.-Y.; Ho, C.-L. *J. Mater. Chem.* **2009**, *19*, 4457–4482. (f) Kamtekar, K. T.; Monkman, A. P.; Bryce, M. R. *Adv. Mater.* **2010**, *22*, 572–582.

(2) For recent examples, see: (a) Sun, Y.; Giebink, N. C.; Kanno, H.; Ma, B.; Thompson, M. E.; Forrest, S. R. *Nature* **2006**, *440*, 908–912. (b) Qin, T.; Ding, J.; Wang, L.; Baumgarten, M.; Zhou, G.; Müllen, K.

J. Am. Chem. Soc. **2009**, *131*, 14329–14336. (c) Bolink, H. J.; De Angelis, F.; Baranoff, E.; Klein, C.; Fantacci, S.; Coronado, E.; Sessolo, M.; Kalyanasundaram, K.; Grätzel, M.; Nazeeruddin, M. K. *Chem. Commun.* **2009**, 4672–4674. (d) Su, S.-J.; Gonmori, E.; Sasabe, H.; Kido, J. *Adv. Mater.* **2008**, *20*, 4189–4194. (e) Ding, J.; Gao, J.; Cheng, Y.; Xie, Z.; Wang, L.; Ma, D.; Jing, X.; Wang, F. *Adv. Funct. Mater.* **2006**, *16*, 575–581. (f) Kwong, R. C.; Lamansky, S.; Thompson, M. E. *Adv. Mater.* **2000**, *12*, 1134–1138.

(3) (a) DeRosa, M. C.; Hodgson, D. J.; Enright, G. D.; Dawson, B.; Evans, C. E. B.; Crutchley, R. J. *J. Am. Chem. Soc.* **2004**, *126*, 7619–7626. (b) Thomas, S. W.; Yagi, S.; Swager, T. M. *J. Mater. Chem.* **2005**, *15*, 2829–2835. (c) Borisov, S. M.; Klimant, I. *Anal. Chem.* **2007**, *79*, 7501–7509. (d) Bolink, H. J.; Coronado, E.; Santamaria, S. G.; Sessolo, M.; Evans, N.; Klein, C.; Baranoff, E.; Kalyanasundaram, K.; Grätzel, M.; Nazeeruddin, M. K. *Chem. Commun.* **2007**, 3276–3278. (e) Mak, C. S. K.; Pentlehner, D.; Stich, M.; Wolfbeis, O. S.; Chan, W. K.; Yersin, H. *Chem. Mater.* **2009**, *21*, 2173–2175.

(4) (a) Schmittel, M.; Lin, H. W. *Inorg. Chem.* **2007**, *46*, 9139–9145. (b) Zhao, Q.; Liu, S. J.; Li, F. Y.; Yi, T.; Huang, C. H. *Dalton Trans.* **2008**, 3836–3840.

(5) (a) Lo, K. K. W.; Hui, W. K.; Chung, C. K.; Tsang, K. H. K.; Ng, D. C. M.; Zhu, N. Y.; Cheung, K. K. *Coord. Chem. Rev.* **2005**, *249*, 1434–1450. (b) Lau, J. S. Y.; Lee, P. K.; Tsang, K. H. K.; Ng, C. H. C.; Lam, Y. W.; Cheng, S. H.; Lo, K. K. W. *Inorg. Chem.* **2009**, *48*, 708–718. (c) Zhang, K. Y.; Lo, K. K. W. *Inorg. Chem.* **2009**, *48*, 6011–6025. (d) Jiang, W.; Gao, Y.; Sun, Y.; Ding, F.; Xu, Y.; Bian, Z.; Li, F.; Bian, J.; Huang, C. *Inorg. Chem.* **2010**, *49*, 3252–3260.

(6) (a) Adachi, C.; Baldo, C. M. A.; Thompson, M. E.; Forrest, S. R. *J. Appl. Phys.* **2001**, *90*, 5048–5051. (b) Baldo, M. A.; O'Brien, D. F.; You, Y.; Shoustikov, A.; Sibley, S.; Thompson, M. E.; Forrest, S. R. *Nature* **1998**, *395*, 151–154. (c) O'Brien, D. F.; Baldo, M. A.; Thompson, M. E.; Forrest, S. R. *Appl. Phys. Lett.* **1999**, *74*, 442–444.

(7) (a) Sajoto, T.; Djurovich, P. I.; Tamayo, A. B.; Oxgaard, J.; Goddard, W. A.; Thompson, M. E. *J. Am. Chem. Soc.* **2009**, *131*, 9813–9822. (b) Endo, A.; Suzuki, K.; Yoshihara, T.; Tobita, S.; Yahiro, M.; Adachi, C. *Chem. Phys. Lett.* **2008**, *460*, 155–157. (c) Kawamura, Y.; Goushi, K.; Brooks, J.; Brown, J. J.; Sasabe, H.; Adachi, C. *Appl. Phys. Lett.* **2005**, *86*, 071104. (d) Holzer, W.; Penzkofer, A.; Tsuboi, T. *Chem. Phys.* **2005**, *308*, 93–102. (e) Tanaka, I.; Tabata, Y.; Tokito, S. *Jpn. J. Appl. Phys., Part 2* **2004**, *43*, L1601–L1603.

(8) (a) Lee, S. J.; Park, K.-M.; Yang, K.; Kang, Y. *Inorg. Chem.* **2009**, *48*, 1030–1037. (b) Ho, C.-L.; Wong, W.-Y.; Gao, Z.-Q.; Chen, C.-H.; Cheah, K.-W.; Yao, B.; Xie, Z.; Wang, Q.; Ma, D.; Wang, L.; Yu, X.-M.; Kwok, H.-S.; Lin, Z. *Adv. Funct. Mater.* **2008**, *18*, 319–331. (c) Zhou, G.; Wong, W.-Y.; Yao, B.; Xie, Z.; Wang, L. *Angew. Chem., Int. Ed.* **2007**, *46*, 1149–1151. (d) Sajoto, T.; Djurovich, P. I.; Tamayo, A.; Yousufuddin, M.; Bau, R.; Thompson, M. E. *Inorg. Chem.* **2005**, *44*, 7992–8003. (e) Tsuboyama, A.; Iwawaki, H.; Furugori, M.; Mukaide, T.; Kamatani, J.; Igawa, S.; Moriyama, T.; Miura, S.; Takiguchi, T.; Okada, S.; Hoshino, M.; Ueno, K. *J. Am. Chem. Soc.* **2003**, *125*, 12971–12979.

(9) King, K. A.; Spellane, P. J.; Watts, R. J. *J. Am. Chem. Soc.* **1985**, *107*, 1431–1432.

(10) Tamayo, A. B.; Alleyne, B. D.; Djurovich, P. I.; Lamansky, S.; Tsyba, I.; Ho, N. N.; Bau, R.; Thompson, M. E. *J. Am. Chem. Soc.* **2003**, *125*, 7377–7387.

(11) (a) Lee, C.-L.; Lee, K. B.; Kim, J.-J. *Appl. Phys. Lett.* **2000**, *77*, 2280–2282. (b) Chen, F.-C.; Yang, Y.; Thompson, M. E.; Kido, J. *Appl. Phys. Lett.* **2002**, *80*, 2308–2310. (c) Gong, X.; Robinson, M. R.; Ostrowski, J. C.; Moses, D.; Bazan, G. C.; Heeger, A. J. *Adv. Mater.* **2002**, *14*, 581–585. (d) Lamansky, S.; Djurovich, P. I.; Abdel-Razzaq, F.; Garon, S.; Murphy, D. L.; Thompson, M. E. *J. Appl. Phys.* **2002**, *92*, 1570–1575. (e) Zhu, W.; Mo, Y.; Yuan, M.; Yang, W.; Cao, Y. *Appl. Phys. Lett.* **2002**, *80*, 2045–2047. (f) Yang, X. H.; Neher, D.; Scherf, U.; Bagnich, S. A. *J. Appl. Phys.* **2003**, *93*, 4413–4419. (g) Yang, X.; Neher, D.; Hertel, D.; Däubler, T. K. *Adv. Mater.* **2004**, *16*, 161–165. (h) Yang, X. H.; Neher, D. *Appl. Phys. Lett.* **2004**, *84*, 2476–2478. (i) Gong, X.; Moses, D.; Heeger, A. J. *J. Phys. Chem. B* **2004**, *108*, 8601–8605.

(12) (a) Sandee, A. J.; Williams, C. K.; Evans, N. R.; Davies, J. E.; Boothby, C. E.; Köhler, A.; Friend, R. H.; Holmes, A. B. *J. Am. Chem. Soc.* **2004**, *126*, 7041–7048. (b) Evans, N. R.; Devi, L. S.; Mak, C. S. K.; Watkins, S. E.; Pascu, S. I.; Köhler, A.; Friend, R. H.; Williams, C. K.; Holmes, A. B. *J. Am. Chem. Soc.* **2006**, *128*, 6647–6656.

(13) (a) Tavasli, M.; Bettington, S.; Bryce, M. R.; Al Attar, H. A.; Dias, F. B.; King, S.; Monkman, A. P. *J. Mater. Chem.* **2005**, *15*, 4963–4970. (b) Bettington, S.; Tavasli, M.; Bryce, M. R.; Batsanov, A. S.; Thompson, A. L.; Al Attar, H. A.; Dias, F. B.; Monkman, A. P. *J. Mater. Chem.* **2006**, *16*, 1046–1052. (c) Bettington, S.; Tavasli, M.; Bryce, M. R.; Beeby, A.; Al-Attar, H.; Monkman, A. P. *Chem.—Eur. J.* **2007**, *13*, 1423–1431. (d) Tavasli, M.; Bettington, S.; Perepichka, I. F.; Batsanov, A. S.; Bryce, M. R.; Rothe, C.; Monkman, A. P. *Eur. J. Inorg. Chem.* **2007**, 4808–4814. (e) Zeng, X. S.; Tavasli, M.; Perepichka, I. F.; Batsanov, A. S.; Bryce, M. R.; Chiang, C. J.; Rothe, C.; Monkman, A. P. *Chem.—Eur. J.* **2008**, *14*, 933–943.

(14) (a) Jiang, J. X.; Xu, Y. H.; Yang, W.; Guan, R.; Liu, Z. Q.; Zhen, H. Y.; Cao, Y. *Adv. Mater.* **2006**, *18*, 1769–1773. (b) Zhang, Y.; Xu, Y.; Niu, Q.; Peng, J.; Yang, W.; Zhu, X.; Cao, Y. *J. Mater. Chem.* **2007**, *17*, 992–1001.

(15) Schulz, G. L.; Chen, X.; Chen, S.-A.; Holdcroft, S. *Macromolecules* **2006**, *39*, 9157–9165.

(16) (a) Wang, X.-Y.; Kimyonok, A.; Weck, M. *Chem. Commun.* **2006**, 3933–3935. (b) Wang, X.-Y.; Prabhu, R. N.; Schmehl, R. H.; Weck, M. *Macromolecules* **2006**, *39*, 3140–3146.

(17) (a) Hwang, S.; Moorefield, C. N.; Newkome, G. R. *Chem. Soc. Rev.* **2008**, *37*, 2543–2557. (b) Lo, S.-C.; Male, N. A. H.; Markham, J. P. J.; Magennis, S. W.; Burn, P. L.; Salata, O. V.; Samuel, I. D. W. *Adv. Mater.* **2002**, *14*, 975–979. (c) Cumpstey, N.; Bera, R. N.; Burn, P. L.; Samuel, I. D. W. *Macromolecules* **2005**, *38*, 9564–9570. (d) Zhou, G.; Wong, W.; Yao, B.; Xie, Z.; Wang, L. *Angew. Chem., Int. Ed.* **2007**, *46*, 1149–1151. (e) Ding, J.; Lü, J.; Cheng, Y.; Xie, Z.; Wang, L.; Jing, X.; Wang, F. *Adv. Funct. Mater.* **2008**, *18*, 2754–2762. (f) Zhou, G.-J.; Wong, W.-Y.; Yao, B.; Xie, Z.; Wang, L. *J. Mater. Chem.* **2008**, *18*, 1799–1809. (g) Knights, K. A.; Stevenson, S. G.; Shipley, C. P.; Lo, S.-C.; Olsen, S.; Harding, R. E.; Gambino, S.; Burn, P. L.; Samuel, I. D. W. *J. Mater. Chem.* **2008**, *18*, 2121–2130.

(18) Schulz, G. L.; Holdcroft, S. *Chem. Mater.* **2008**, *20*, 5351–5355.

(19) (a) Xu, Y.; Peng, J.; Jiang, J.; Xu, W.; Yang, W.; Cao, Y. *Appl. Phys. Lett.* **2005**, *87*, 193502–193504. (b) King, S. M.; Al-Attar, H. A.; Evans, R. J.; Congreve, A.; Beeby, A.; Monkman, A. P. *Adv. Funct. Mater.* **2006**, *16*, 1043–1050.

(20) DeRosa, M. C.; Hodgson, D. J.; Enright, G. D.; Dawson, B.; Evans, C. E. B.; Crutchley, R. J. *J. Am. Chem. Soc.* **2004**, *126*, 7619–7626.

(21) The single crystal of Ir(*m*-Brppy) was not obtained (see Figure S1 for ^{1}H NMR spectrum), and its facial configuration was inferred from the fact that all studied bromo-substituted Ir(ppy)$_3$ complexes were prepared under similar conditions.

(22) Allen, F. H.; Kennard, O. *Chem. Des. Autom. News* **1993**, *8*, 31–37.

(23) Jo, J. H.; Chi, C. Y.; Hoger, S.; Wegner, G.; Yoon, D. Y. *Chem.—Eur. J.* **2004**, *10*, 2681–2688.

(24) *Handbook of Photochemistry*; Montalti, M., Credi, A., Prodi, L., Gandolfi, M., Eds.; Taylor & Francis: Boca Raton, FL, 2006.

(25) (a) Tang, K. C.; Liu, K. L.; Chen, I. C. *Chem. Phys. Lett.* **2004**, *386*, 437–441. (b) Hedley, G. J.; Ruseckas, A.; Samuel, I. D. W. *Chem. Phys. Lett.* **2008**, *450*, 292–296.

(26) (a) Haskins-Glusac, K.; Pinto, M. R.; Tan, C.; Schanze, K. S. *J. Am. Chem. Soc.* **2004**, *124*, 14964–14971. (b) Glusac, K.; Ko1se, M. E.; Jiang, H.; Schanze, K. S. *J. Phys. Chem. B* **2007**, *111*, 929–940.

(27) Geng, Y.; Trajkovska, A.; Katsis, D.; Ou, J. J.; Culligan, S. W.; Chen, S. H. *J. Am. Chem. Soc.* **2002**, *124*, 8337–8347.

(28) Hay, P. J. *J. Phys. Chem. A* **2002**, *106*, 1634–1641.

(29) Rausch, A. F.; Thompson, M. E.; Yersin, H. *J. Phys. Chem. A* **2009**, *113*, 5927–5932.

(30) (a) Caspar, J. V.; Kober, E. M.; Sullivan, B. P.; Meyer, T. J. *J. Am. Chem. Soc.* **1982**, *104*, 630–632. (b) Caspar, J. V.; Meyer, T. J. *J. Phys. Chem.* **1983**, *87*, 952–957.

(31) Cheng, Y.-M.; Li, E. Y.; Lee, G.-H.; Chou, P.-T.; Lin, S.-Y.; Shu, C.-F.; Hwang, K.-C.; Chen, Y.-L.; Song, Y.-H.; Chi, Y. *Inorg. Chem.* **2007**, *46*, 10276–10286.

(32) Li, J.; Djurovich, P. I.; Alleyne, B. D.; Yousufuddin, M.; Ho, N. N.; Thomas, J. C.; Peters, J. C.; Bau, R.; Thompson, M. E. *Inorg. Chem.* **2005**, *44*, 1713–1727.

(33) Frisch, M. J.; et al. *Gaussian 2003, Revision C.02*; Gaussian, Inc.: Pittsburgh, PA, 2003.

(34) (a) Becke, A. D. *Phys. Rev. A* **1988**, *38*, 3098–3100. (b) Lee, C.; Yang, W.; Parr, G. G. *Phys. Rev. B* **1988**, *37*, 785–789.

(35) Francl, M. M.; Pietro, W. J.; Hehre, W. J.; Binkley, J. S.; Gordon, M. S.; Defrees, D. J.; Pople, J. A. *J. Chem. Phys.* **1982**, *77*, 3654–3665.

(36) (a) Hay, P. J.; Wadt, W. R. *J. Chem. Phys.* **1985**, *82*, 270–283. (b) Wadt, W. R.; Hay, P. J. *J. Chem. Phys.* **1985**, *82*, 284. (c) Hay, P. J.; Wadt, W. R. *J. Chem. Phys.* **1985**, *82*, 299–310.

(37) Chi, C. Y.; Im, C.; Wegner, G. *J. Chem. Phys.* **2006**, *124*, 024907.